arXiv:1410.8743v1 [cond-mat.supr-con] 31 Oct 2014

Highly textured oxypnictide superconducting thin films on metal substrates

Kazumasa Iida,[1, a)] Fritz Kurth,[1] Masashi Chihara,[2] Naoki Sumiya,[2] Vadim Grinenko,[1] Ataru Ichinose,[3] Ichiro Tsukada,[3] Jens Hänisch,[1] Vladimir Matias,[4] Takafumi Hatano,[2] Bernhard Holzapfel,[5] and Hiroshi Ikuta[2]

[1)] *Institute for Metallic Materials, IFW Dresden, D-01171 Dresden, Germany*

[2)] *Department of Crystalline Materials Science, Nagoya University, Chikusa, Nagoya 464-8603, Japan*

[3)] *Central Research Institute of Electric Power Industry, 2-6-1 Nagasaka, Yokosuka, Kanagawa 240-0196, Japan*

[4)] *iBeam Materials, Inc., 2778A Agua Fria Street, Santa Fe, NM 87507, U.S.A.*

[5)] *Karlsruhe Institute of Technology, Institute for Technical Physics, Hermann von Helmholtz-Platz 1, D-76344 Eggenstein-Leopoldshafen, Germany*

(Dated: 3 November 2014)

Highly textured NdFeAs(O,F) thin films have been grown on ion beam assisted deposition (IBAD)-MgO/Y_2O_3/Hastelloy substrates by molecular beam epitaxy. The oxypnictide coated conductors showed a superconducting transition temperature (T_c) of 43 K with a self-field critical current density (J_c) of 7.0×10^4 A/cm^2 at 5 K, more than 20 times higher than powder-in-tube processed SmFeAs(O,F) wires. Albeit higher T_c as well as better crystalline quality than Co-doped $BaFe_2As_2$ coated conductors, in-field J_c of NdFeAs(O,F) was lower than that of Co-doped $BaFe_2As_2$. These results suggest that grain boundaries in oxypnictides reduce J_c significantly compared to that in Co-doped $BaFe_2As_2$ and, hence biaxial texture is necessary for high J_c.

PACS numbers: 74.70.Xa, 81.15.Fg, 74.78.-w, 74.25.Sv, 74.25.F-

Electron or hole doped $AEFe_2As_2$ (AE =Ba and Sr) and Fe(Se,Te) show high upper critical fields with low anisotropies at low temperatures that offer a unique possibility for high field magnet applications[1,2]. Thanks to the recent progress of processing technology, powder-in-tube (PIT) processed $AEFe_2As_2$ yields high performance of in-field critical current density (J_c)[3–5]. Furthermore, Co-doped $BaFe_2As_2$ and Fe(Se,Te) on ion beam assisted deposition (IBAD)-MgO/Y_2O_3/Hastelloy with comparable J_c to those on single crystalline substrates have been demonstrated, although the texture quality of the formers is inferior to the latters[6–9]. These results indicate that J_c properties are quite robust against grain boundaries (GBs) in those materials. Indeed, the critical angle for Co-doped $BaFe_2As_2$ at which J_c starts to being degraded is twice as large as cuprates[10,11].

On the other hand, LnFeAs(O,F) (Ln =Sm, Nd) is expected to have potentially higher J_c than other Fe-based superconductors due to the highest T_c around 55 K[12,13] among the Fe-based superconductors except for monolayer FeSe[14]. However, the level of J_c in PIT-processed SmFeAs(O,F) wire is around 4.0×10^3 A/cm^2 even in low fields at 4.2 K[15], much lower than $AEFe_2As_2$ wires[3–5]. A fundamental reason for the low J_c in oxypnictide may be due to higher sensitivity against the grain misorientation than other Fe-based superconductors, since LnFeAs(O,F) (Ln =Sm, Nd) has more anisotropic crystal structure and superconducting properties, which resembles high-T_c cuprates. Those facts imply that biaxial textured forms are necessary for high J_c, indicating that the 2nd generation $YBa_2Cu_3O_7$ coated conductor technology might be suitable for realizing oxypnictide superconducting wires. However, no studies on oxypnictide coated conductors have been reported to date due presumably to the difficulties in fabricating epitaxial LnFeAs(O,F) thin films on technical substrates.

Here we report on a preparation of NdFeAs(O,F) thin films on MgO-templated Hastelloy by means of molecular beam epitaxy (MBE). By comparing with similar studies on Co-doped $BaFe_2As_2$ coated conductors[6], we point out the necessity of biaxial texture in oxypnictide wires and tapes for high J_c.

The NdFeAs(O,F) thin films were prepared on IBAD-MgO/Y_2O_3/Hastelloy by MBE. The IBAD-MgO/Y_2O_3/Hastelloy has been provided by iBeam Materials, Inc[16]. A mother compound of NdFeAsO was deposited on MgO templated Hastelloy, followed by the deposition of a NdOF cap layer for F diffusion to the NdFeAsO layer. The detailed fabrication can be found in Ref. 17. The respective thickness of NdFeAs(O,F) superconducting layer, MgO template and Y_2O_3 buffer layer were approximately 90 nm, 180 nm and 10 nm confirmed by cross-sectional transmission electron microscope (TEM), which will be shown later.

Phase purity and texture quality of the films were examined by x-ray diffraction (Fig. 1). The $\theta/2\theta$-scan, fig. 1 (a), shows $00l$ reflections of NdFeAs(O,F) and NdOF together with the 002 reflection of MgO, indicative of c-axis texturing. Albeit the film was c-axis oriented, NdAs, FeAs and unidentified impurity phase were detected. The ω-scan for the 005 reflection of NdFeAs(O,F) in fig. 1 (b) shows a full width at half maximum (FWHM, $\Delta\omega$) of 1.72°, which is a simi-

[a)] Electronical address: iida@nuap.nagoya-u.ac.jp; Present address: Department of Crystalline Materials Science, Nagoya University, Chikusa, Nagoya 464-8603, Japan

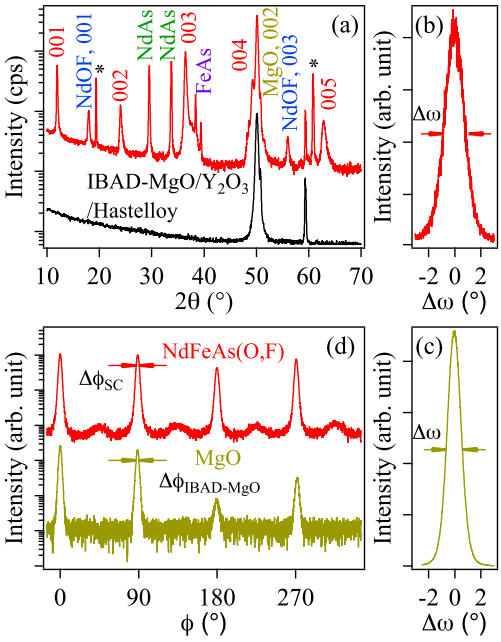

FIG. 1. (Color online) Summary of structural characterization by x-ray diffraction: (a) the $\theta/2\theta$ - scans in Bragg-Brentano geometry using Co-K_α radiation. The red and black traces are NdFeAs(O,F) coated conductor and IBAD-MgO/Y_2O_3/Hastelloy substrate, respectively. Unindentified phase is marked by a star. (b) The 005 rocking curve of NdFeAs(O,F) using Cu-K_α radiation. (c) The 002 rocking curve of MgO. (d) The 102 ϕ-scans of NdFeAs(O,F) and the 220 ϕ-scans of MgO measured in a texture goniometer operating with Cu-K_α radiation.

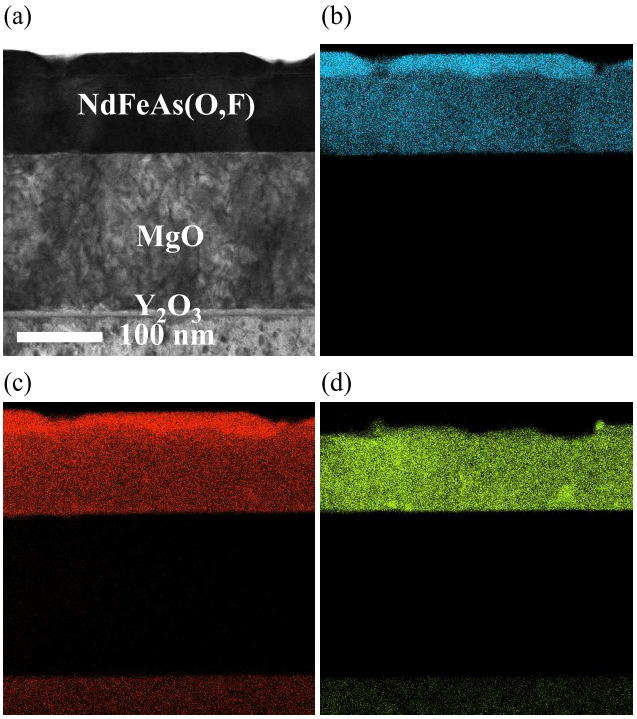

FIG. 2. (Color online) (a) Cross-sectional scanning TEM image of the NdFeAs(O,F) thin film. The respective thickness of NdFeAs(O,F) superconducting layer, MgO template and Y_2O_3 buffer layer are approximately 90 nm, 180 nm and 10 nm. (b) Elemental Nd, (c) F, and (d) Fe mappings measured by energy dispersive x-ray spectroscopy.

lar value to the textured MgO template[($\Delta\omega = 1.24°$), fig. 1 (c)]. The 102 ϕ-scans of NdFeAs(O,F) reveal a small amount of 45° in-plane rotated grains, as shown in fig. 1 (d). However, the main reflections were observed at every 90°, indicative of highly biaxial textured NdFeAs(O,F) films. Here, the epitaxial relation is identified as (001)[100]NdFeAs(O,F)‖(001)[100]MgO. The average $\Delta\phi$ of NdFeAs(O,F) and MgO are 3.38° and 2.88°, respectively. Hence $\Delta\omega$ and $\Delta\phi$ of NdFeAs(O,F) are similar to those of the underlying MgO template, indicating that the texture is well transferred to NdFeAs(O,F). We have also confirmed that the NdOF cap layer is biaxially textured and its epitaxial relation is (001)[110]NdOF‖(001)[100]NdFeAs(O,F), which is an observation similar to SmFeAs(O,F) thin films[18].

In order to check the homogeneity of the NdFeAs(O,F), microstructural investigation by TEM together with elemental mappings were carried out (fig. 2). In the superconducting layer, some areas have different contrast, which originates from misoriented grains transferred from the underlying MgO templates. As can be seen in fig. 3(a), the MgO layer with white and black in-contrast yields different types of NdFeAs(O,F) grains (i.e., texture transferring from the buffer layer). It is further obvious from fig. 2(a) that trapezoid shaped NdOF layer was grown on NdFeAs(O,F), which is proved by the elemental mappings shown in fig. 2(b) and (c) [i.e., high concentration of both Nd and F] and x-ray $\theta/2\theta$ - scan shown in fig. 1 (a). Whilst Nd is homogeneous in the superconducting layer, Fe is segregated in the vicinity of the interface [fig. 2 (d)]. Although it is less clear, we note that the area where Fe is segregated seems to be also rich in F.

Shown in fig. 3(b) is the high-resolution TEM image of the NdFeAs(O,F) thin film in the vicinity of the MgO textured template / NdFeAs(O,F) film interface. Clearly a relatively sharp interface is observed between NdFeAs(O,F) and MgO, which is similar to the Co-doped Ba-122 and Fe(Se,Te) thin films on MgO single crystalline substrates prepared by pulsed laser deposition[19,20]. These results indicate that MgO single crystalline substrates or textured MgO templates are suitable for epitaxial growth of Fe-based superconducting thin films, similarly to CaF_2 substrate[13,21–23].

The NdFeAs(O,F) film exhibits a T_c of 43 K at which spliting between zero field-cooled (ZFC) and field-cooled (FC) branches of the normalized magnetization curves $-m(T)/m(8.5\,\mathrm{K})$ is observed as shown in fig. 4(a). Here magnetic measurements have been carried out by

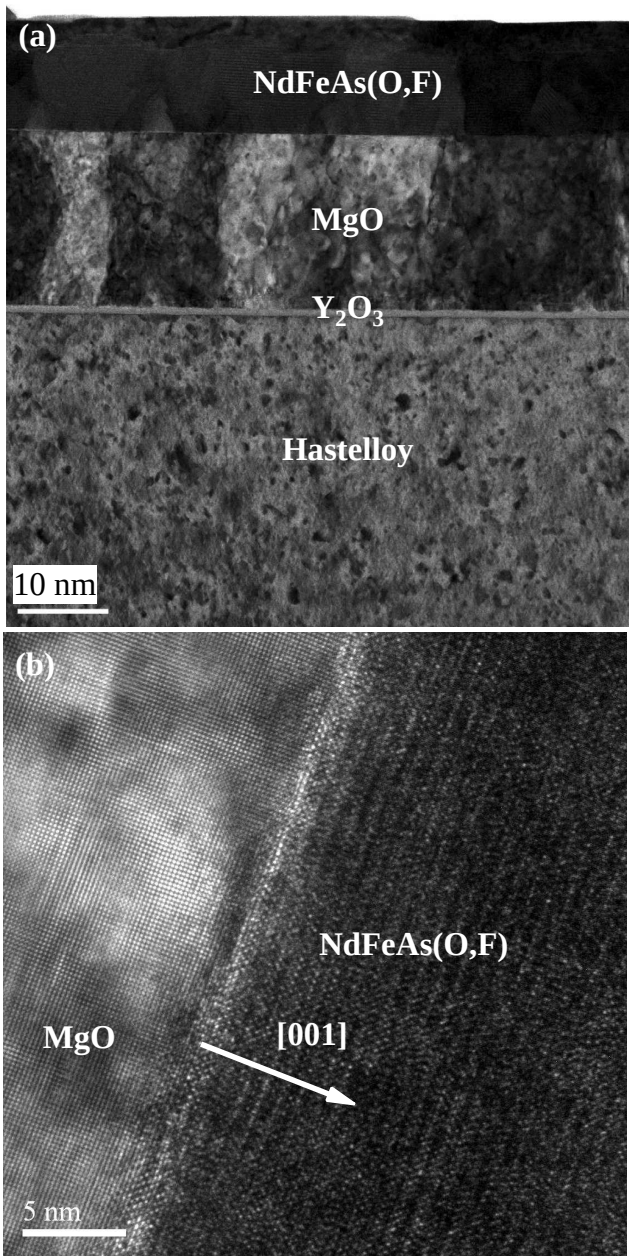

FIG. 3. (a) Cross-sectional scanning TEM image of the NdFeAs(O,F) thin film, which is an area different from fig. 2(a). (b) High-resolution TEM image of the NdFeAs(O,F) thin film in the vicinity of the MgO textured template / NdFeAs(O,F) film interface.

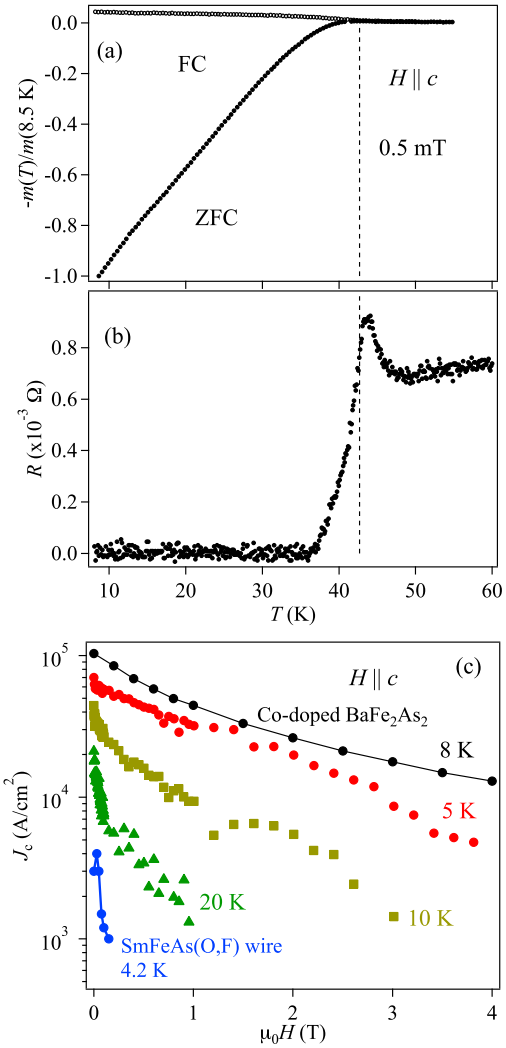

FIG. 4. (Color online) (a) The normalized magnetization curves $-m(T)/m(8.5\,\mathrm{K})$ of the NdFeAs(O,F) coated conductor for zero field-cooled (ZFC) and field-cooled (FC) branches measured by a SQUID magnetometer. A small magnetic field of 0.5 mT was applied parallel to the c-axis of the film. The data were normalized to the ZFC value at 8.5 K. (b) The transport measurements for the same film conducted in a PPMS by a four-probe method. (c) The $J_c - H$ properties of NdFeAs(O,F) for $H \parallel c$ measured in a SQUID magnetometer. In-field transport J_c of Co-doped $BaFe_2As_2$ coated conductor and PIT-processed SmFeAs(O,F) wire are also plotted in the same figure for comparison[6,15].

means of a superconducting quantum interference device (SQUID, Quantum Design) magnetometer and the data were normalized to the ZFC value at 8.5 K. On the other hand, zero resistance was observed at 37 K, measured in a Physical Property Measurement System (PPMS, Quantum Design) by a four-probe method [fig. 4(b)]. This difference is due to a large bias current of 100 mA, leading to a shift of zero resistance temperature to lower temperatures. A sudden increase in the resistance before the superconducting transition is a general observation for films on conducting substrates, where the resistivity of the films in the normal state is higher than that of the substrates[24].

Shown in fig. 4(c) is in-field J_c property of the NdFeAs(O,F) coated conductor measured by a magnetization method using a SQUID magnetometer. Magnetic J_c was evaluated by the following formula: $J_c = \frac{20\Delta m}{(a-a^2/3b)V}$, where Δm is the difference between the magnetic mo-

TABLE I. The average FWHM values ($\Delta\phi_{SC}$) of NdFeAs(O,F), Co-doped $BaFe_2As_2$ on IBAD-MgO/Y_2O_3/Hastelloy and IBAD-MgO. The data for Co-doped $BaFe_2As_2$ were taken from Ref.6. The respective reflections for NdFeAs(O,F), Co-doped $BaFe_2As_2$ and MgO are 102, 103 and 220.

Films	$\Delta\phi_{SC}$	$\Delta\phi_{IBAD-MgO}$
NdFeAs(O,F)	3.38°	2.88°
Co-doped $BaFe_2As_2$	5.13°	5.98°

ments observed in the magnetic hysteresis loops for increasing and decreasing field cycles, a and b are the film dimensions for the ab-plane, and V is the superconducting volume[25]. As can be seen in fig. 4(c), the self-field J_c of NdFeAs(O,F) coated conductor reaches 7.0×10^4 A/cm^2 at 5 K, which is more than 20 times higher than PIT-processed SmFeAs(O,F)[15]. Additionally, the oxypnictide coated conductor shows better in-field performance than PIT-processed SmFeAs(O,F). However, J_c of NdFeAs(O,F) film on MgO single crystalline substrate exceeds 10^4A/cm^2 even at 35 T ($H \parallel c$) at 4.2 K[26], indicating that there is much room for optimization. Compared to the Co-doped $BaFe_2As_2$ coated conductor[6], the level of J_c for NdFeAs(O,F) is relatively low. Note that the zero resistance temperature of Co-doped $BaFe_2As_2$ is 17.5 K, much lower than that of NdFeAs(O,F). Furthermore, in-field J_c for Co-doped $BaFe_2As_2$ shown in fig. 4(c) was measured at 8 K. By considering the same reduced temperature (i.e., $t = T/T_{c,0} = 8/17.5 = 0.457$ for Co-doped $BaFe_2As_2$), one can expect that J_c of NdFeAs(O,F) at 16.9 K, which is supposed to be located between the curves measured at 10 and 20 K, is reduced significantly by only small magnetic fields. It is also worth mentioning that the $\Delta\phi$ value of NdFeAs(O,F) is smaller than that of Co-doped $BaFe_2As_2$[6], as shown in Table I. These results indicate that NdFeAs(O,F) shows weak-link behavior, which necessitates biaxial texture for high J_c. Nevertheless bicrystal experiments on LnFeAs(O,F) are necessary to quantitatively characterize the GBs properties.

In summary, textured NdFeAs(O,F) thin films have been realized on IBAD-MgO/Y_2O_3/Hastelloy substrates by MBE. The oxypnictide coated conductors showed a T_c of 43 K with a self-field J_c of 7.0×10^4 A/cm^2 at 5 K, more than 20 times higher than PIT processed SmFeAs(O,F) wires. However, the current-limiting effects by GBs in LnFeAs(O,F) seem to be more serious than in AEFe$_2$As$_2$ and Fe(Se,Te). Hence it is necessary to align grains biaxially in oxypnictide wires and tapes for high J_c.

ACKNOWLEDGMENTS

The authors thank M. Kühnel and U. Besold for their technical support. The research leading to these results has received funding from European Union's Seventh Framework Programme (FP7/2007-2013) under grant agreement number 283141 (IRON-SEA). This research has been also supported by Strategic International Collaborative Research Program (SICORP), Japan Science and Technology Agency.

[1] M. Putti, I. Pallecchi, E. Bellingeri, M. R. Cimberle, M. Tropeano, C. Ferdeghini, A. Palenzona, C. Tarantini, A. Yamamoto, J. Jiang, J. Jaroszynski, F. Kametani, D. Abraimov, A. Polyanskii, J. D. Weiss, E. E. Hellstrom, A. Gurevich, D. C. Larbalestier, R. Jin, B. C. Sales, A. S. Sefat, M. A. McGuire, D. Mandrus, P. Cheng, Y. Jia, H. H. Wen, S. Lee, and C. B. Eom, Supercond. Sci. Technol. **23**, 034003 (2010).
[2] Q. Li, W. Si, and I. K. Dimitrov, Rep. Prog. Phys. **74**, 124510 (2011).
[3] J. D. Weiss, C. Tarantini, J. Jiang, F. Kametani, A. A. Polyanskii, D. C. Larbalestier, and E. E. Hellstrom, Nat. Mater. **11**, 682 (2012).
[4] Z. Gao, Y. Ma, C. Yao, X. Zhang, C. Wang, D. Wang, S. Awaji, and K. Watanabe, Sci. Rep. **2**, 998 (2012).
[5] Z. Gao, K. Togano, A. Matsumoto, and H. Kumakura, Sci. Rep. **4**, 4065 (2014).
[6] K. Iida, J. Hänisch, S. Trommler, V. Matias, S. Haindl, F. Kurth, I. L. del Pozo, R. Hühne, M. Kidszun, J. Engelmann, L. Schultz, and B. Holzapfel, Appl. Phys. Express **4**, 013103 (2011).
[7] T. Katase, H. Hiramatsu, V. Matias, C. Sheehan, Y. Ishimaru, T. Kamiya, K. Tanabe, and H. Hosono, Appl. Phys. Lett. **98**, 242510 (2011).
[8] W. Si, S. J. Han, X. Shi, S. N. Ehrlich, J. Jaroszynski, A. Goyal, and Q. Li, Nat. Commun. **4**, 1347 (2013).
[9] S. Trommler, J. Hänisch, V. Matias, R. Hühne, E. Reich, K. Iida, S. Haindl, L. Schultz, and B. Holzapfel, Supercond. Sci. Technol. **25**, 084019 (2012).
[10] T. Katase, Y. Ishimaru, A. Tsukamoto, H. Hiramatsu, T. Kamiya, K. Tanabe, and H. Hosono, Nat. Commun. **2**, 409 (2011).
[11] K. Iida, S. Haindl, F. Kurth, J. Hänisch, L. Schultz, and B. Holzapfel, Physics Procedia **45**, 189 (2013).
[12] Z. A. Ren, W. Lu, J. Yang, W. Yi, X. L. Shen, Z. C. Li, G. C. Che, X. L. Dong, L. L. Sun, F. Zhou, and Z. X. Zhao, Chin. Phys. Lett. **25**, 2215 (2008).
[13] H. Uemura, T. Kawaguchi, T. Ohno, M. Tabuchi, T. Ujihara, Y. Takeda, and H. Ikuta, Solid State Commun. **152**, 735 (2012).
[14] S. He, J. He, W. Zhang, L. Zhao, D. Liu, X. Liu, D. Mou, Y. Ou, Q. Wang, Z. Li, L. Wang, Y. Peng, Y. Liu, C. Chen, L. Yu, G. Liu, X. Dong, J. Zhang, C. Chen, Z. Xu, X. Chen, X. Ma, Q. Xue, and X. J. Zhou, Nat. Mater. **12**, 605 (2013).
[15] M. Fujioka, T. Kota, M. Matoba, T. Ozaki, Y. Takano, H. Kumakura, and Y. Kamihara, Appl. Phys. Express **4**, 063102 (2011).
[16] C. Sheehan, Y. Jung, T. Holesinger, D. M. Feldmann, C. Edney, J. F. Ihlefeld, P. G. Clem, and V. Matias, Appl. Phys. Lett. **98**, 071907 (2011).
[17] T. Kawaguchi, H. Uemura, T. Ohno, M. Tabuchi, T. Ujihara, Y. Takeda, and H. Ikuta, Appl. Phys. Express **4**, 083102 (2011).
[18] K. Iida, J. Hänisch, C. Tarantini, F. Kurth, J. Jaroszynski, S. Ueda, M. Naito, A. Ichinose, I. Tsukada, E. Reich, V. Grinenko, L. Schultz, and B. Holzapfel, Sci. Rep. **3**, 2139 (2013).
[19] M. Hanawa, A. Ichinose, S. Komiya, I. Tsukada, Y. Imai, and A. Maeda, Jpn. J. Appl. Phys. **51**, 010104 (2012).
[20] H. Hiramatsu, T. Katase, Y. Ishimaru, A. Tsukamoto, T. Kamiya, K. Tanabe, and H. Hosono, Mat. Sci. Eng. B **177**, 515 (2012).
[21] I. Tsukada, M. Hanawa, T. Akiike, F. Nabeshima, Y. Imai, A. Ichinose, S. Komiya, T. Hikage, T. Kawaguchi, H. Ikuta, and A. Maeda, Appl. Phys. Express **4**, 053101 (2011).
[22] F. Kurth, E. Reich, J. Hänisch, A. Ichinose, I. Tsukada, R. Hühne, S. Trommler, J. Engelmann, L. Schultz, B. Holzapfel, and K. Iida, Appl. Phys. Lett. **102**, 142601 (2013).

[23] A. Ichinose, I. Tsukada, F. Nabeshima, Y. Imai, A. Maeda, F. Kurth, B. Holzapfel, K. Iida, S. Ueda, and M. Naito, Appl. Phys. Lett. **104**, 122603 (2014).
[24] S. Trommler, R. Hühne, J. Hänisch, E. Reich, K. Iida, S. Haindl, V. Matias, L. Schultz, and B. Holzapfel, Appl. Phys. Lett. **100**, 122602 (2012).
[25] D. X. Chen and R. B. Goldfarb, J. Appl. Phys. **66**, 2489 (1989).
[26] C. Tarantini, F. Kurth, M. Chihara, N. Sumiya, J. Jaroszynski, J. Hänisch, H. Takafumi, K. Iida, and H. Ikuta, Unpublished.